

CCUS: 4433310

Investigating CO₂ Plume Dynamics in Deep Saline Aquifers during Geologic CO₂ Sequestration Using Simulation and Data-Driven Models.

Maliha Anzuman*¹, Aaditya Khanal^{1,2}, Nagu Daraboina¹, 1. Russell School of Chemical Engineering, The University of Tulsa, 2. McDougall School of Petroleum Engineering, The University of Tulsa

Copyright 2026, Carbon Capture, Utilization, and Storage conference (CCUS) DOI 10.15530/ccus-2026-4433310

This paper was prepared for presentation at the Carbon Capture, Utilization, and Storage conference held in The Woodlands, TX, 30 March – 01 April.

The CCUS Technical Program Committee accepted this presentation on the basis of information contained in an abstract submitted by the author(s). The contents of this paper have not been reviewed by CCUS and CCUS does not warrant the accuracy, reliability, or timeliness of any information herein. All information is the responsibility of, and, is subject to corrections by the author(s). Any person or entity that relies on any information obtained from this paper does so at their own risk. The information herein does not necessarily reflect any position of CCUS. Any reproduction, distribution, or storage of any part of this paper by anyone other than the author without the written consent of CCUS is prohibited.

Abstract

Carbon dioxide (CO₂) trapping and long-term containment in deep saline aquifers are controlled by complex interaction among multiphase flow processes, geological heterogeneity, and capillary effects. Although structural trapping can retain a large fraction of injected supercritical CO₂, excessive structural accumulation beneath the caprock may increase the risk of caprock integrity loss and pressure-induced failure. Inadequate representation of geological and flow uncertainties can therefore lead to overestimation of structurally trapped CO₂ and underestimation of residual and dissolution trapping mechanisms. The objective of this study is to systematically quantify reservoir-scale CO₂ trapping over time while accounting for key geological and multiphase flow uncertainties and to identify conditions that can reduce CO₂ accumulation beneath the caprock while enhancing the other trapping mechanisms. To achieve this, a compositional reservoir simulator was employed to model ten years of supercritical CO₂ injection and ninety years of post-injection observation in a heterogeneous reservoir. Reservoir heterogeneity was captured through multiple geostatistical realizations of porosity and permeability, while permeability anisotropy (k_v/k_h) was explicitly incorporated to represent uncertainty in vertical and lateral migration of CO₂. As capillary pressure and relative permeability exhibit substantial variability, even within the same rock type, we took different unique combinations of pore entry pressure (P_{ce}), pore size distribution index (λ), initial brine saturation (S_{wi}), residual gas saturation (S_{gr}) and hysteresis effects. 796 data were generated by simulation and used to train Random Forest and XGBoost models to predict free, residually trapped and dissolved CO₂. XGBoost showed better performance, achieving R^2 values of 0.958, 0.969, and 0.978 for dissolved, trapped, and free CO₂ during post injection period and 0.982, 0.982, and 0.821 at long-term storage times, respectively. Sensitivity analysis reveals that permeability anisotropy and residual gas

saturation are the dominant controls on CO₂ mobility and residual trapping, while capillary entry pressure strongly governs dissolution trapping after injection and free CO₂ at longer times. Initial water saturation, pore size distribution, and reservoir heterogeneity exhibit secondary but physically consistent influences that diminish as the system approaches equilibrium. These results highlight the strong time dependence of CO₂ trapping mechanisms and demonstrate that explicitly accounting for multiphase-flow uncertainty significantly improves long-term storage security while reducing reliance on structural trapping alone.

Keywords: Capillary Pressure; CCS; Reservoir Simulation; CO₂ Plume; Relative permeability.

Introduction

Carbon capture, Utilization and Storage (CCUS) is recognized as a critical engineering solution for effective carbon management. As reported in the Global Status of CCS 2025, there are 77 operational CCS facilities running currently which is 54% more than 2024 with ability to capture 64 Mtpa of CO₂ [1]. With this continuity, CCUS is expected to contribute nearly 15% to the total emissions reduction by 2070 [2]. Deep saline aquifers are considered as large-scale storage for their massive storage capacity, moderate porosity and permeability, stable and extensive worldwide distribution. CO₂ is captured and injected into deep saline aquifers in a supercritical state, as its density is considerably higher than that of gaseous CO₂ [3,4], enabling more CO₂ to be stored per unit pore volume and significantly improving storage efficiency. Then it starts to move upward through the aquifer until structurally trapped beneath an impermeable caprock with high capillary entry pressure [5]. At the same time, some CO₂ becomes immobilized through residual trapping, where it remains as disconnected ganglia within pore spaces due to capillary forces, wettability, and the pore structure of the reservoir [6]. Over longer timescales, CO₂ gradually dissolves into brine, enhancing storage security through convective mixing, while mineral reactions slowly convert CO₂ into stable carbonates, providing permanent storage and potentially altering reservoir porosity and permeability [3,7–9]. Among all of them, structural trapping poses the highest risk due to mobile CO₂, whereas residual and solubility trapping are safer mechanisms [10].

During injecting CO₂ into deep saline aquifers many factors need to be considered such as site investigation, economic aspects, monitoring, risks [11]. Experimental and physics-based numerical simulations are the widely used tools to properly understand the influence of reservoir uncertainties and multiphase flow processes so that CO₂ plume migration can be predicted over time and the risk of CO₂ leakage can be reduced. Several researchers have reached conclusions of CO₂ storing process through simulation by analyzing petrophysical properties. Such as, CO₂ can be stored easily if a reservoir has low to medium heterogeneity [12]. Vertical permeability is the most significant parameter for predicting how much CO₂ stays trapped or can move through the rock and porosity is the most important factor that affects how much CO₂ can be dissolved in the rock over time [13]. CO₂ injectivity and CO₂ trapping depends on the combined influence of reservoir properties (permeability, k_v/k_h) and flow related petrophysical parameters (S_{gr} , S_{wi} , λ , S_{g_critic} , Max CO₂ K_r) [14]. Capillary pressure plays a critical role in CO₂ sequestration by promoting the trapping of CO₂ through dissolution into formation water and mineralization. Neglecting capillary effects results in nearly half of the injected CO₂ remaining in a mobile phase, reducing storage efficiency [8]. Physics-based simulations further show that variation in capillary pressure curve can affect the CO₂ plume behavior, with capillary entry pressure being the dominant factor governing plume geometry [11]. As capillary behavior is closely related to wettability, recent data-driven studies have shown that contact angle can be predicted with high accuracy and interpretability, with temperature and mineralogical composition as dominant controlling factors [15].

This study provides a systematic and physically consistent assessment of CO₂ plume migration and trapping by jointly evaluating the coupled effects of reservoir heterogeneity, capillary pressure, relative permeability and hysteresis across both post-injection and long-term storage period. Rather than treating these controls separately, the proposed framework demonstrates how their relative importance evolves with time and emerges from nonlinear interactions between buoyancy, capillarity, and multiphase flow history.

By combining compositional simulations with machine-learning-based feature attribution, this work not only identifies the dominant parameters governing free, residually trapped, and dissolved CO₂, but also explains the underlying physical mechanisms responsible for their influence.

Methodology

An isothermal 2D compositional model is developed using CMG-GEM (v2025.10) to investigate CO₂ plume migration and long-term sequestration in a deep saline aquifer. The model represents a heterogeneous sandstone reservoir vertically confined by low-permeability shale layers. It consists of 8120 Cartesian grid blocks (203x1x40) with a lateral extent of 1000 m and a top depth of 1700 m, discretized into 40 layers of 2.5 m thickness, as shown in **Figure 1(a)**. A centrally located vertical injection well injects supercritical CO₂ over 1797–1800 m for 10 years at 100 m³/day, subject to a maximum bottom-hole pressure of 44.5 MPa. Although this flow rate is lower than field-scale operations, this produces a pore-volume-normalized injection intensity comparable to or higher than representative 3D CCUS studies [16,17] and is therefore appropriate for the reduced near-wellbore-focused 2D model domain. The simulation is extended to 100 years to evaluate post-injection behavior. Reservoir heterogeneity is generated using a stationary Gaussian random field, with permeability sampled from a lognormal distribution (mean 200 mD, $C_v = 0.4$) and porosity computed from an empirical correlation given in Eq (1) [18]:

$$K_h = 7x10^7(\varphi^{9.61}) \quad (1)$$

A total of 20 different realizations of porosity and permeability were generated based on different correlation length uncertainty of the reservoir and to assess their impact on final CO₂ retention. The vertical permeability remains the same as horizontal permeability for the base case. The reservoir properties and input parameters used in the saline aquifer model are summarized in **Table 1**. The water-gas contact is set at the top of the reservoir, resulting in an initially fully brine-saturated system [19]. The aquifer is initialized at the pressure of 17000 kPa and a constant temperature of 75°C.

Reservoir properties	Values	References
Reservoir temperature (°C)	75	Current study
Max. Bottomhole pressure (kPa)	44500	[8]
Grid number	8120 (203×1×40)	Current study
Lateral extent (m)	1000	Current study
Thickness (m)	100	Current study
Depth at the top (m)	1700	[20]
Permeability (mD)	200	[20–22]
Porosity	0.265	Current Study
Fluid pressure (kPa)	17,000	[22]
CO ₂ injection rate(m ³ /D)	100	Current study

Table 1— Summary of reservoir properties

To describe both the relative permeability and capillary pressure curve, we employed the Brooks- Corey model [23]:

$$k_{rw} = (S_w^*)^{N_w} \quad (2)$$

$$k_{r,co_2} = k_{r,co_2}(S_{wi})[1 - S_w^*]^2[1 - (S_w^*)^{N_{co_2}}] \quad (3)$$

$$S_w^* = \frac{(S_w - S_{wi})}{(1 - S_{wi})} \quad (4)$$

$$P_c = P_{ce} \times \left(\frac{S_w - S_{wi}}{1 - S_{wi}} \right)^{-\frac{1}{\lambda}} \quad (5)$$

where k_{rw} and k_{r,co_2} represent the water relative permeability and the gas relative permeability respectively, S_w^* is the effective water saturation, S_{wi} is the irreducible water saturation. N_w and N_{CO_2} are Corey exponents for water and CO₂, respectively. In this work, values of 9 and 4 were used for N_w and N_{CO_2} while for $k_{r,co_2}(S_{wi})$, a value of 0.95 was assumed based on the experimental evaluations of the Mt. Simon sandstone [23]. P_c and P_{ce} represent the capillary pressure and the capillary entry pressure respectively where λ is the pore saturation index. For the base case study, the pore saturation index, λ is set to 0.80, the pore entry pressure, P_{ce} is 166 kPa and the initial water saturation, S_{wi} is taken 0.259. To account for uncertainty in capillary and relative permeability behavior, a total of 60 realizations were generated by randomly sampling combinations of these parameters within the ranges: λ between 0.4-0.8, P_{ce} between 1-200 kPa and S_{wi} between 0.11-0.5 [11,14,23]. The Land trapping model is applied to capture the hysteresis effects in the relative permeability of CO₂. A base-case residual gas saturation ($S_{gr}=0.25$) was assumed, with sensitivity analyses spanning 0.15–0.40. **Figure 1 (b) and (c)** illustrate the base-case relative permeability and capillary pressure, enabling systematic evaluation of capillary pressure, relative permeability, and hysteresis effects on CO₂ trapping during drainage-imbibition cycles.

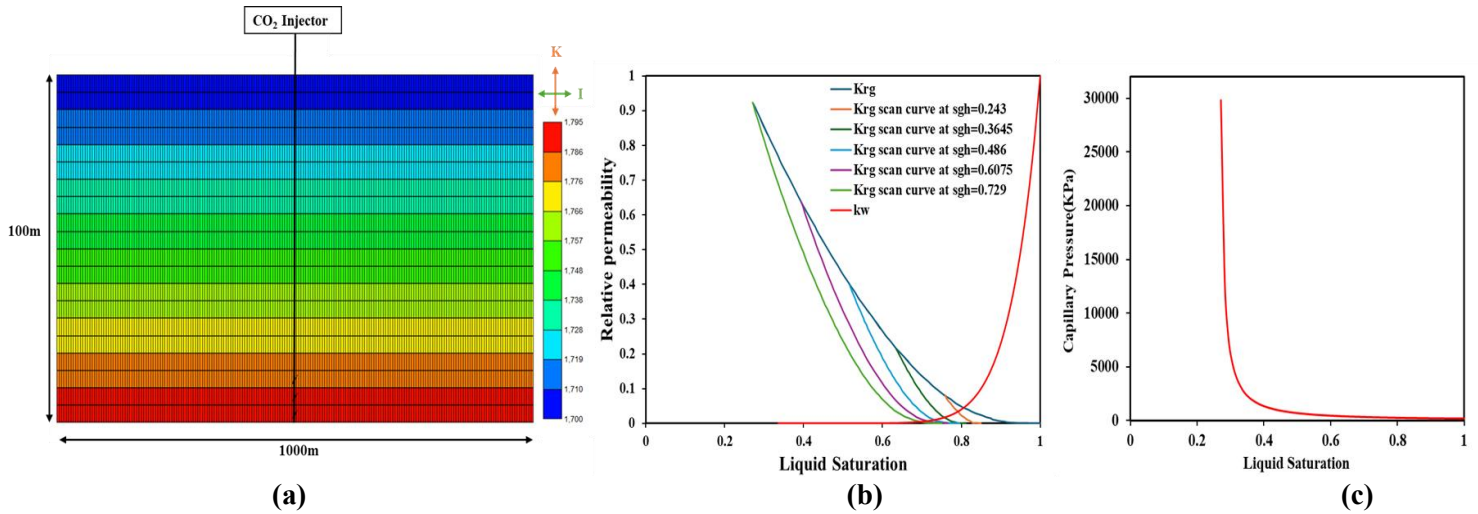


Figure 1. (a) An IK view of 2D reservoir, where the color scale represents the reservoir depth measured from the surface (b) Relative permeability and (c) Capillary pressure curve (base case).

Phase behavior and thermophysical properties of the reservoir fluids are modeled using CMG-WinProp (version 2025.10), with the formation initially assumed to be fully water-saturated. Henry's law constant is calculated as a function of reservoir pressure and temperature using Harvey's correlation [24]. Gas density is estimated using the Peng-Robinson equation of state [25], while fluid viscosity and aqueous-phase density were determined using the correlation proposed by Rowe and Chou and Kestin et al. [26,27], respectively. **Table 2** shows all the parameters ranges used for the sensitivity analysis for this study.

Parameter	Reason for parameter selection	Values	References
k_v/k_h	This uncertain parameter determines whether CO ₂ spreads laterally and gets trapped or rises vertically and threatens the caprock.	0.02-1	[28,29]

Correlation length	Controls spatial continuity of porosity and permeability (avg-200 mD) and CO ₂ plume migration. 20 realizations were generated with correlation lengths of 1–40 grid cells.	4.93-98.52m	Current Study
Pore saturation index, λ	An uncertain constitutive-model parameter, known as phase interference parameter, that controls the curvature of wetting phase relative permeability model and influences CO ₂ plume geometry.	0.4-0.8	[30,31]
Pore entry pressure	An uncertain capillary parameter representing the minimum pressure required for CO ₂ to enter the pore network and controls the onset of non-wetting phase invasion.	1-200 KPa	[30–32]
Residual gas saturation	An uncertain multiphase-flow parameter that directly controls residual trapping efficiency and long-term immobilization of CO ₂ .	0.15-0.4	[30,33]
Initial water saturation	An uncertain reservoir-state parameter that determines the initial availability of pore space for CO ₂ injection, influences relative permeability and capillary pressure behavior, and directly affects CO ₂ mobility and residual trapping efficiency.	0.11-0.5	[14,23]

Table 1—Critical parameters and the reasons to choose them for the sensitivity analysis.

Random Forest combines multiple regression trees trained in bootstrapped data and random feature subsets to improve prediction stability and reduce overfitting, whereas XGBoost is a boosting algorithm that sequentially trains decision trees by optimizing a gradient-based loss function to correct error from predicting trees [34,35]. A total of 796 simulation runs were used to evaluate the influence of reservoir parameters on CO₂ trapping. These runs represent the subset of simulations that achieved full numerical convergence over the 100-year temporal domain, with the remaining cases discarded due to convergence failures induced by randomized capillary pressure thresholds and steep aqueous phase relative permeability curve. The dataset was used to train and validate Random Forest (RF) and XGBoost models to predict dissolved, residually trapped, and free CO₂. Data was split into 80% training and 20% testing, with grid-search hyperparameter optimization and five-fold cross-validation using R^2 as the evaluation metric. CMOST captures the coupled effects of relative permeability hysteresis and capillary pressure, while the trained ML models isolate the individual impacts of S_{wi} , λ , and P_{ce} on CO₂ trapping mechanisms.

Results and Discussions

CO₂ was injected for 10 years and monitored over a 90-year post-injection period, with analysis focused on dissolution, residual, and free-phase trapping. Results indicate that the controlling influence of reservoir parameters on CO₂ trapping evolves substantially from the early post-injection stage to long-term storage. To capture this temporal shift, CO₂ plume behavior was evaluated at 20 years and 100 years. **Figure 2** illustrates the spatial distribution of CO₂ global mole fraction at these times, highlighting contrasting plume evolution patterns.

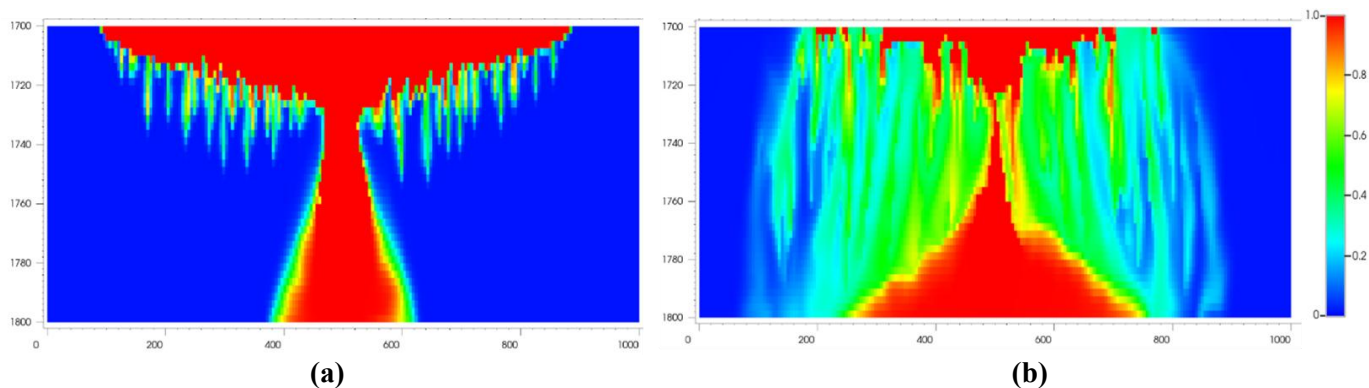


Figure 2. Distribution of global mole fraction of CO₂ over time. (a) 20 years (b) 100 years

Figure 3 illustrates the cross-validated predictions of dissolved, trapped and free CO₂ for different combinations of randomized input parameters. As shown in Figure 3, the XGBoost model exhibits slightly better predictive performance compared to Random Forest. For 100 years case, XGBoost model achieved good predictive accuracy, with R^2 values of 0.982, 0.982, 0.821 for dissolved, trapped and free CO₂, respectively, outperforming Random Forest ($R^2=0.968, 0.976$ and 0.777) Similarly, for 20 years case XGBoost yielded higher accuracy ($R^2 = 0.958, 0.969, 0.978$) for dissolved, trapped and free CO₂ compared to Random Forest ($R^2 = 0.937, 0.971, 0.951$) The R^2 value of free CO₂ (year-100) is less than the value of year 20. As simulation time increases, free CO₂ progressively diminishes due to dissolution and residual trapping, leading to fewer valid data points for model training and consequently lower R^2 values for free CO₂ predictions.

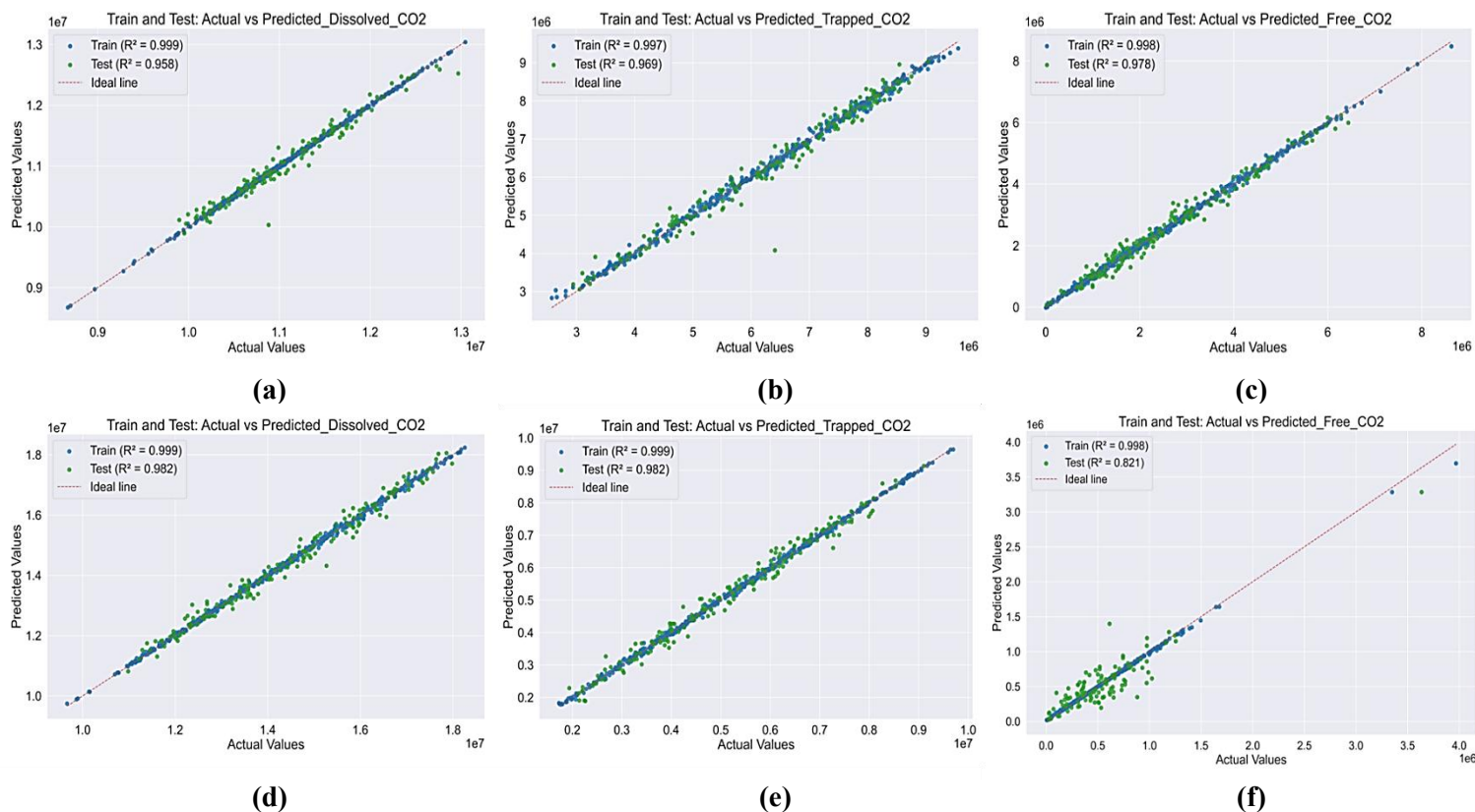


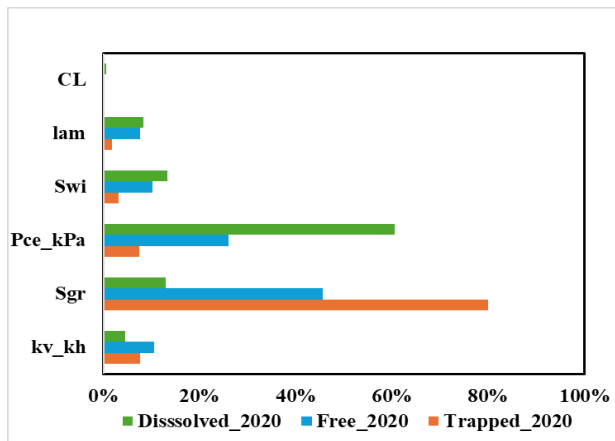
Figure 3. Performance of XGBoost model for predicting CO₂ (a) Dissolved_year_20, (b) Trapped_year_20, (c) Free_year_20 and (d) Dissolved_year_100, (e) Trapped_year_100, (f) Free_year_100.

Finally, XGBoost feature-importance analysis and tornado plots were used to identify key controlling parameters and their proportional or inverse effects on CO₂ plume behavior; **Figure 4** presents the results for dissolved, trapped, and free CO₂.

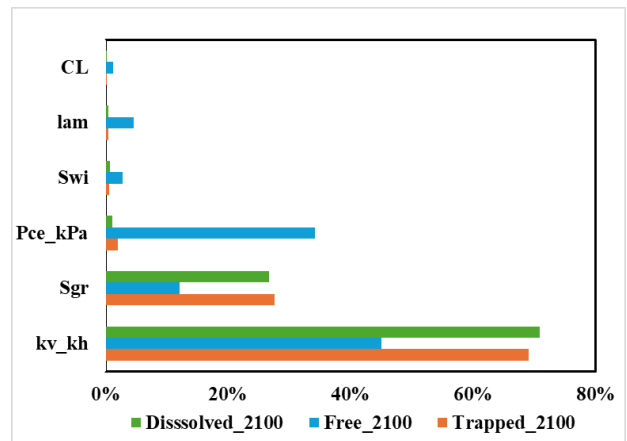
Permeability (k_v/k_h) primarily controls free CO₂ behavior by regulating vertical migration. Higher k_v/k_h promotes upward CO₂ movement, limiting lateral plume spread and reducing brine contact, which lowers residual and dissolved CO₂ during and shortly after injection. After 100 years, CO₂ accumulation beneath the caprock enhances brine interaction and convective mixing, increasing dissolution and reducing free CO₂. Consequently, k_v/k_h emerges as the dominant control on dissolved, residually trapped, and free CO₂, with importance values of 0.70, 0.69, and 0.45, respectively, as shown in **Figure 4b**.

Capillary entry pressure (P_{ce}) controls the balance between buoyancy-driven flow and capillary resistance, exerting first-order control on CO₂ plume extent. Higher P_{ce} requires greater pressure for CO₂ to invade smaller pores, restricting upward migration and forcing lateral spreading. This slower, more tortuous flow increases CO₂ residence time, enhancing residual trapping and promoting dissolution during the post-injection period. Over long-term storage, as buoyancy weakens, high P_{ce} continues to limit vertical migration, reducing free CO₂ while sustaining residual trapping and limiting further dissolution. Consequently, P_{ce} is the second most influential parameter governing free CO₂ at late times and dissolved CO₂ during the post-injection period.

A moderate effect of initial water saturation can be seen in post injection period. A higher S_{wi} means that a larger portion of pore throats remain water-filled after injection ends, which restricts the continuity of the CO₂ phase. As a result, the relative permeability crossover point shifts to higher water saturation, delaying and limiting the formation of connected CO₂ flow pathways. With reduced connectivity, the CO₂ plume loses mobility more rapidly, leading to a decline in free CO₂ during the post-injection phase. At the same time, the dominance of the water phase promotes capillary snap-off and imbibition, breaking the CO₂ plume into disconnected ganglia that become immobilized as residually trapped CO₂. In addition, higher S_{wi} corresponds to a larger brine volume and longer gas-water contact time once injection stops, which enhances diffusive and convective mass transfer of CO₂ into the aqueous phase. Over prolonged time after injection, the influence of S_{wi} gradually weakens as the system approaches equilibrium.



(a)



(b)

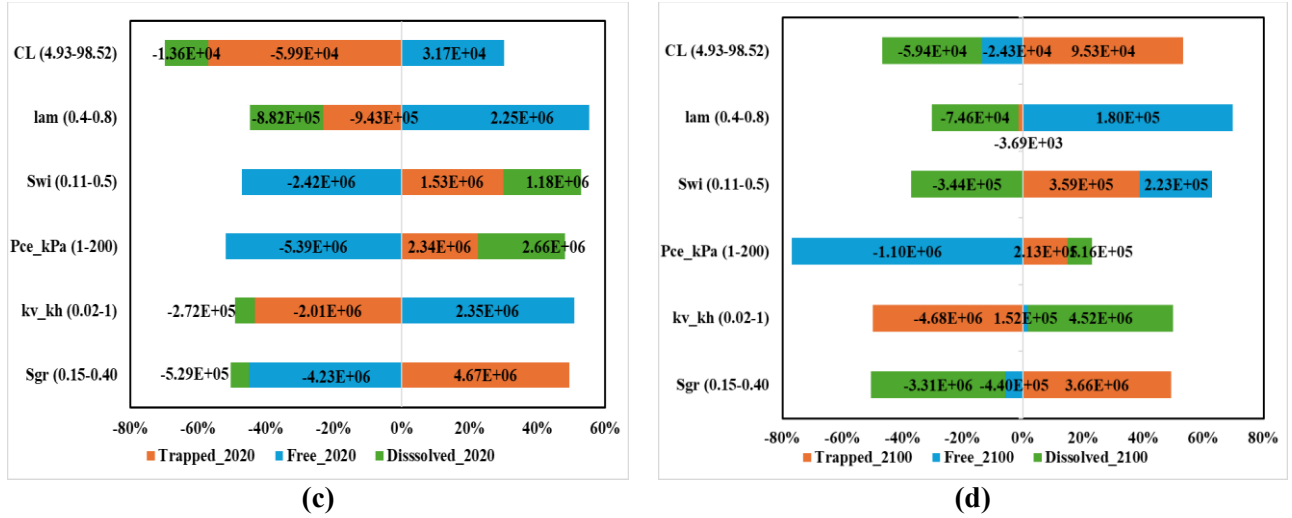


Figure 4. Feature importance plot (a) for year_20, (b) for year_100 and Tornado plot (c) for year_20, (d) for year_100.

As shown in **Figure 4(a)**, Residual gas saturation (S_{gr}) is the most influential parameter controlling free CO₂ and residual trapping during post injection period with important factors of 0.45, 0.8, respectively and it remains the second most influential parameter governing dissolved and trapped CO₂ over longer time periods. After injection ends, the system transitions from drainage to imbibition as brine re-enters CO₂-filled pores. A higher S_{gr} indicates stronger hysteresis, meaning a larger fraction of CO₂ becomes immobilized during imbibition due to snap-off and pore-scale disconnection. As a result, trapped CO₂ increases immediately after injection, while free CO₂ decreases because the connected gas pathways collapse. At the same time, dissolution is reduced because the immobilized CO₂ has limited mobility and reduced effective contact with flowing brine. Over longer periods, the impact of S_{gr} on trapping becomes less pronounced because most residual trapping has already occurred early in the imbibition process.

Conclusions

This study presents an integrated physics-based and data-driven framework to investigate CO₂ plume migration and long-term trapping in a heterogeneous deep saline aquifer. CMG-GEM simulations capturing multiphase CO₂-brine flow, capillary pressure, relative permeability, and hysteresis under reservoir uncertainty were coupled with Random Forest and XGBoost models to analyze large datasets and quantify the relative importance of key parameters controlling free, residually trapped, and dissolved CO₂ during post-injection and long-term storage. The main findings are summarized below-

- CO₂ trapping behavior is strongly time-dependent, with parameter influence differing between the post injection period and longer-term storage.
- Permeability anisotropy (k_v/k_h) exerts the strongest control on free CO₂ by regulating vertical plume migration and interaction with brine and becomes increasingly influential for all trapping mechanisms over long times.
- Residual gas saturation (S_{gr}) is the most influential for free CO₂ and residual trapping immediately after injection, due to strong relative permeability hysteresis and imbibition-driven snap-off and remains the second most influential parameter for dissolved and trapped CO₂ at later times.
- Capillary entry pressure (P_{ce}) governing the balance between buoyancy-driven flow and capillary resistance is the most impactful parameter for dissolved CO₂ in post injection period with importance factor of 0.61 and in prolonged time P_{ce} has a greater influence on free CO₂.

- Initial water saturation, pore size distribution and reservoir heterogeneity show secondary influences on CO₂ trapping. Higher S_{wi} reduces free CO₂ and enhances residual and dissolution trapping early on, while a larger pore size distribution promotes early CO₂ mobility but less important over time. Because heterogeneity was introduced solely through correlation-length variations while maintaining constant mean porosity and permeability, it primarily altered plume geometry and migration pathways rather than the total pore volume or capillary-controlled trapping capacity, resulting in a comparatively weaker influence on CO₂ trapping volumes.
- Among the machine learning models, XGBoost consistently outperforms Random Forest, achieving high predictive accuracy for dissolved, trapped and free CO₂, particularly during the post injection period.

Future work should extend this framework to fully three-dimensional, multilayered reservoirs with explicit caprock representation, while incorporating end point saturation uncertainty and dynamic wettability effects to improve physical realism. Expanding late-time free CO₂ datasets would enhance machine learning accuracy, and integration with field scale monitoring data would strengthen applicability for practical CO₂ storage assessment and risk evaluation.

Acknowledgments

We gratefully acknowledge the U.S. Department of Energy, Office of Science, Basic Energy Sciences Geoscience program under Award Number DE-SC0025695. Any opinions, findings, and conclusions or recommendations expressed in this material are those of the author(s) and do not necessarily reflect the views of the funding agency.

References

- [1] Global Status of CCS, (2025). <https://www.globalccsinstitute.com/global-status-of-ccs/> (accessed November 12, 2025).
- [2] IEA, CCUS in the Transition to Net-Zero Emissions, 2023.
- [3] A. Khanal, M.F. Shahriar, Physics-Based Proxy Modeling of CO₂ Sequestration in Deep Saline Aquifers, *Energies* 2022, Vol. 15, Page 4350 15 (2022) 4350. <https://doi.org/10.3390/EN15124350>.
- [4] M. Hamed, E. Shirif, Numerical Reservoir Simulation of CO₂ Storage in Saline Aquifers: Assessment of Trapping Mechanisms, Geochemistry, O₂ Impurities and Brine Salinity, *Processes* 14 (2026) 316. <https://doi.org/10.3390/pr14020316>.
- [5] N.M. Burnside, M. Naylor, Review and implications of relative permeability of CO₂/brine systems and residual trapping of CO₂, *International Journal of Greenhouse Gas Control* 23 (2014) 1–11. <https://doi.org/10.1016/j.ijggc.2014.01.013>.
- [6] Q. Zhang, S. Geiger, J.E.A. Storms, D. V. Voskov, M.D. Jackson, G.J. Hampson, C. Jacquemyn, A.W. Martinius, Capillary pinning in sedimentary rocks for CO₂ storage: Mechanisms, terminology and State-of-the-Art, *International Journal of Greenhouse Gas Control* 144 (2025) 104385. <https://doi.org/10.1016/J.IJGGC.2025.104385>.
- [7] M.F. Shahriar, A. Khanal, Effect of Formation Heterogeneity on CO₂ Dissolution in Subsurface Porous Media, *ACS Earth Space Chem.* 7 (2023) 2073–2090. <https://doi.org/10.1021/ACSEARTHSPACECHEM.3C00175>.
- [8] A. Khanal, M. Irfan Khan, M. Fahim Shahriar, Comprehensive parametric study of CO₂ sequestration in deep saline aquifers, *Chem. Eng. Sci.* 287 (2024). <https://doi.org/10.1016/j.ces.2024.119734>.
- [9] P.N.Y.M. Otabir, A. Khanal, F. Nath, Geochemical Impacts of CO₂ Mineralization in Carbonate and Basalt Formations: A Critical Review on Challenges and Future Outlook, *Energy & Fuels* 39 (2025) 1226–1251. <https://doi.org/10.1021/acs.energyfuels.4c04424>.

- [10] L. Nghiem, V. Shrivastava, B. Kohse, M. Hassam, C. Yang, Simulation and Optimization of Trapping Processes for CO₂ Storage in Saline Aquifers, *Journal of Canadian Petroleum Technology* 49 (2010) 15–22. <https://doi.org/10.2118/139429-PA>.
- [11] H. Wu, N. Lubbers, H.S. Viswanathan, R.M. Pollyea, A multi-dimensional parametric study of variability in multi-phase flow dynamics during geologic CO₂ sequestration accelerated with machine learning, *Appl. Energy* 287 (2021). <https://doi.org/10.1016/j.apenergy.2021.116580>.
- [12] Z. Rasheed, A. Raza, R. Gholami, M. Rabiei, A. Ismail, V. Rasouli, A numerical study to assess the effect of heterogeneity on CO₂ storage potential of saline aquifers, *Energy Geoscience* 1 (2020) 20–27. <https://doi.org/10.1016/J.ENGEOS.2020.03.002>.
- [13] M.I. Khan, A. Khanal, Parametric Study of CO₂ Sequestration in Deep Saline Aquifers Using Data-Driven Models, in: *SPE Western Regional Meeting Proceedings, Society of Petroleum Engineers (SPE)*, 2024. <https://doi.org/10.2118/218906-MS>.
- [14] M. Vitor Barbosa Machado, M. Delshad, K. Sepehrnoori, The Interplay between Experimental Data and Uncertainty Analysis in Quantifying CO₂ Trapping during Geological Carbon Storage, *Clean Energy and Sustainability* 2 (2024) 10001–10001. <https://doi.org/10.35534/ces.2024.10001>.
- [15] Md.S. Rahaman, Md.A. Islam, M.M. Alam, M. Anzuman, Data driven prediction of reservoir rock wettability in shale using deep learning and gene expression programming for CCUS, *Discover Civil Engineering* 3 (2026) 28. <https://doi.org/10.1007/s44290-026-00416-y>.
- [16] S.M. MousaviMirkalaei, M.D. Edmondson, Coupled Geochemistry CCS Modelling: How Much Simplification is Required?, *Offshore Technology Conference Asia, OTCA 2024* (2024). <https://doi.org/10.4043/34698-MS>.
- [17] A.P. Bump, S. Bakhshian, H. Ni, S.D. Hovorka, M.I. Olariu, D. Dunlap, S.A. Hosseini, T.A. Meckel, Composite confining systems: Rethinking geologic seals for permanent CO₂ sequestration, *International Journal of Greenhouse Gas Control* 126 (2023) 103908. <https://doi.org/10.1016/j.ijggc.2023.103908>.
- [18] M.H. Holtz, Residual Gas Saturation to Aquifer Influx: A Calculation Method for 3-D Computer Reservoir Model Construction, *SPE Proceedings - Gas Technology Symposium* (2002) 23–32. <https://doi.org/10.2118/75502-MS>.
- [19] N. Smith, P. Boone, A. Oguntimhin, G. van Essen, R. Guo, M.A. Reynolds, L. Friesen, M.C. Cano, S. O'Brien, Quest CCS facility: Halite damage and injectivity remediation in CO₂ injection wells, *International Journal of Greenhouse Gas Control* 119 (2022) 103718. <https://doi.org/10.1016/J.IJGGC.2022.103718>.
- [20] J.T. Freiburg, M. Amer, K. Henkel, K. Wemmer, G.H. Grathoff, Illitization in the Mt. Simon Sandstone, Illinois Basin, USA: Implications for carbon dioxide storage, *Mar. Pet. Geol.* 146 (2022) 105963. <https://doi.org/10.1016/j.marpetgeo.2022.105963>.
- [21] D.M. Labotka, S. V. Panno, R.A. Locke, J.T. Freiburg, Isotopic and geochemical characterization of fossil brines of the Cambrian Mt. Simon Sandstone and Ironton–Galesville Formation from the Illinois Basin, USA, *Geochim. Cosmochim. Acta* 165 (2015) 342–360. <https://doi.org/10.1016/J.GCA.2015.06.013>.
- [22] B. Shabani, P. Lu, R. Kammer, C. Zhu, B. Shabani, P. Lu, R. Kammer, C. Zhu, Effects of Hydrogeological Heterogeneity on CO₂ Migration and Mineral Trapping: 3D Reactive Transport Modeling of Geological CO₂ Storage in the Mt. Simon Sandstone, Indiana, USA, *Energies* 2022, Vol. 15, 15 (2022). <https://doi.org/10.3390/EN15062171>.
- [23] S.C.M. Krevor, R. Pini, L. Zuo, S.M. Benson, Relative permeability and trapping of CO₂ and water in sandstone rocks at reservoir conditions, *Water Resour. Res.* 48 (2012) 2532. <https://doi.org/10.1029/2011WR010859>.
- [24] A.H. Harvey, Semiempirical Correlation for Henry's Constants over Large Temperature Ranges, *AIChE Journal* 42 (1996) 1491–1494. <https://doi.org/10.1002/aic.690420531>.

- [25] D.-Y. Peng, D.B. Robinson, A New Two-Constant Equation of State, *Industrial & Engineering Chemistry Fundamentals* 15 (1976) 59–64. <https://doi.org/10.1021/i160057a011>.
- [26] J. Kestin, H.E. Khalifa, R.J. Correia, Tables of the dynamic and kinematic viscosity of aqueous NaCl solutions in the temperature range 20–150 °C and the pressure range 0.1–35 MPa, *J. Phys. Chem. Ref. Data* 10 (1981) 71–88. <https://doi.org/10.1063/1.555641>.
- [27] A.M. Rowe, J.C.S. Chou, Pressure-volume-temperature-concentration relation of aqueous sodium chloride solutions, *J. Chem. Eng. Data* 15 (1970) 61–66. <https://doi.org/10.1021/jc60044a016>.
- [28] B. Ren, Local capillary trapping in carbon sequestration: Parametric study and implications for leakage assessment, *International Journal of Greenhouse Gas Control* 78 (2018) 135–147. <https://doi.org/10.1016/J.IJGGC.2018.08.001>.
- [29] A.P. Bump, S. Bakhshian, H. Ni, S.D. Hovorka, M.I. Olariu, D. Dunlap, S.A. Hosseini, T.A. Meckel, Composite confining systems: Rethinking geologic seals for permanent CO₂ sequestration, *International Journal of Greenhouse Gas Control* 126 (2023). <https://doi.org/10.1016/j.ijggc.2023.103908>.
- [30] H. Wu, N. Lubbers, H.S. Viswanathan, R.M. Pollyea, A multi-dimensional parametric study of variability in multi-phase flow dynamics during geologic CO₂ sequestration accelerated with machine learning, *Appl. Energy* 287 (2021). <https://doi.org/10.1016/j.apenergy.2021.116580>.
- [31] H. Wu, R.S. Jayne, R.M. Pollyea, A parametric analysis of capillary pressure effects during geologic carbon sequestration in a sandstone reservoir, *Greenhouse Gases: Science and Technology* 8 (2018) 1039–1052. <https://doi.org/10.1002/ghg.1815>.
- [32] B. Bennion, S. Bachu, Relative Permeability Characteristics for Supercritical CO₂ Displacing Water in a Variety of Potential Sequestration Zones in the Western Canada Sedimentary Basin, *Proceedings - SPE Annual Technical Conference and Exhibition* (2005) 859–873. <https://doi.org/10.2118/95547-ms>.
- [33] A. Alqahtani, X. He, B. Yan, H. Hoteit, Uncertainty Analysis of CO₂ Storage in Deep Saline Aquifers Using Machine Learning and Bayesian Optimization, *Energies (Basel)*. 16 (2023). <https://doi.org/10.3390/en16041684>.
- [34] D. Zhang, L. Qian, B. Mao, C. Huang, B. Huang, Y. Si, A Data-Driven Design for Fault Detection of Wind Turbines Using Random Forests and XGboost, *IEEE Access* 6 (2018) 21020–21031. <https://doi.org/10.1109/ACCESS.2018.2818678>.
- [35] V.N. Vapnik, *The Nature of Statistical Learning Theory*, Springer Science and Business Media LLC, New York, NY, USA New York, NY, USA, 2000.